NANO LETTERS

2004
Vol. 4, No. 12
2331−2335

A Two-Stage Mechanism of Bimetallic Catalyzed Growth of Single-Walled Carbon Nanotubes

Wei-Qiao Deng, Xin Xu, and William A. Goddard, III*

Materials and Process Simulation Center, Division of Chemistry and Chemical Engineering, California Institute of Technology, Pasadena, California 91125

Received August 17, 2004

ABSTRACT

Using quantum mechanics we examined critical steps in the growth of single-walled carbon nanotubes (SWCN) for Ni, Co, Pt, Cu, Cr, Fe, Mo, Rh, Pd, and their combinations. This suggests a two-stage mechanism consisting of nucleation of nanotube growth (determining the number of SWCN) and growth with defect repair (determining the length of SWCN) and suggests simple computational tests for efficacy. This leads to efficacies in the order Ni+Co > Ni+Pt > Ni > Ni+Cu, consistent with experiment. These results suggest that Mo+Ni would be a better bimetallic catalyst than the best current catalyst, Ni+Co.

Single-walled carbon nanotubes (SWCN) were first produced using arc discharge between metal-containing carbon electrodes[1,2] with only modest yield, but laser vaporization techniques[3,4] now lead to high yield (more than 70−90%) of high quality SWCN. In addition, progress has been made in synthesizing SWCN with chemical vapor deposition (CVD),[5−7] allowing control of the diameter with precise positioning on a substrate. Despite the promise, development of effective processes for large-scale production of high-quality SWCN required for commercial applications demands a much better understanding and control of the microscopic mechanisms. Unfortunately, the complexity of the synthetic procedures has made experimental determination of the mechanism very difficult, and this complexity has also frustrated progress in using theory and simulation to understand the mechanism of nanotube growth.[8]

Clearly, the presence of transition metals such as Ni and Co plays an essential role in producing single-walled nanotubes, since eliminating the metals leads only to finite fullerene balls and carbon deposits. Most likely, these metals act as isolated single atom catalytic sites since the concentration of the transition metal catalyst in the graphite material is quite low (<1%) and the growth temperature is too high for significant cluster formation.[9] On the other hand, there are synergetic effects of having two different metals present. For example, Co combined with Bi or Pb led to the broadening of the range of tube diameters (with up to 60 Å diameter for Co + Bi) during arc discharge growth.[10] Moreover, the yield of SWCN for the Ni+Co bimetallic catalyst improves the production by 10−100 times higher than the yield of either Ni or Co alone.[4] However, the role-(s) played by the metal remain quite uncertain, making it difficult to optimize the catalyst (metal and conditions).

Many mechanisms have been suggested but none explain the most salient observations from the experiments, namely: (1) the catalytic efficiency of different metals has the order Ni > Co ≫ Pt ≫ Cu[4] and (2) the catalytic efficiency of bimetallic catalysts follows the order Ni+Co > Ni+Pt ≫ Co+Cu[4] and Ni+Co > Ni+Fe ∼ Ni ≫ Fe.[11]

We consider that the metal atoms would bind most strongly to the exposed edge or a growing tube, which is highly active with isolated sp^2 radical sites containing destabilized π bonds (1,2 benzyne type) in the plane. We consider that there are two likely roles of the metal: (a) nucleation, forming from available precursors a structure onto which carbon molecules and atoms can add to form bucky tubes;[12−13] and (b) growth with defect repair (G-DR), building on the nucleated structure by adding carbon atoms and molecules to build the side walls while eliminating any carbon pentagons that would eventually close off the tube to terminate the growth.

We carried out QM/MM (quantum mechanics combined with molecular mechanics) calculations (as implemented in Jaguar[14]) to examine the two-stage growth model of nanotubes shown in Figure 1. For the nucleation stage we considered a carbon ring cluster with 20 carbon atoms and a bound catalytic atom, fully optimized at the B3LYP/LACVP* level of density functional theory (DFT). For the growth stage we considered a catalytic atom attached to a short carbon nanotube in which ∼27 atoms near the metal

* Corresponding author. E-mail: wag@wag.caltech.edu.

10.1021/nl048663s CCC: $27.50
Published on Web 11/10/2004

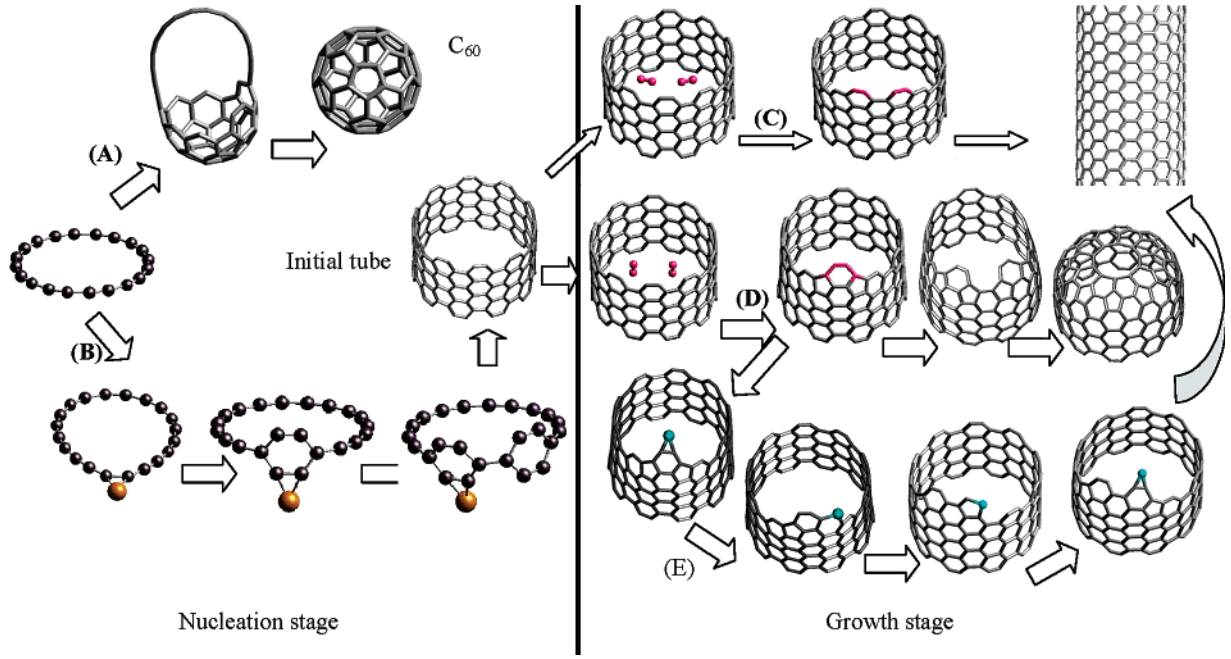

Figure 1. Idealized steps for the two-stage growth model of nanotubes. **Nucleation Stage**: This stage has two distinct types of paths. Path (A): Without a metal the rings lead to formation of C_{60} or fullurenes.[13] Path (B): The metal atom adds to the edge of the polyyne ring to form a site that can catalyze the addition of C_2 to grow the ring into an initial tube.[14] **Growth Stage**: This stage has three distinct types of paths: Path (C) favors forming a nanotube by direct parallel addition of C_2 at the growth edge; Path (D) forms a 5,5,6,6 defect (that would lead to tube closure) by direct vertical addition of C_2 at the growth edge, which, without a metal present, is 1.30 eV more favorable than path (C); Path (E) anneals the 5,5,6,6 defect with the assistance of catalytic metal atoms.

are described with QM at the B3LYP/LACVP* level while another ~138 carbon atoms are described using the Dreiding force field.[15]

First we test the two-stage model by considering the role of Ni, Co, Pt, and Cu on both growth stages.

(A) Nucleation of Nanotubes. We assume that the nucleation stage of nanotube formation proceeds as follows (see Figure 2). (1) The first step is forming a suitable carbon ring and then attaching an appropriate metal atom to the edge of the ring, forming a bridging site that causes the carbon ring structure to twist out of plane as in species (A). A Diels−Alder like addition of a C_2 molecule to (A) forms a hexagonal ring as in (B). (2) The metal atom then migrates along the carbon ring, passing through structures such as (C) and (D) to form the twisted ring geometry as in (E). (3) The structure (E) is ready for another C_2 molecule to do the Diels−Alder addition, forming a second hexagonal ring as (F). These three steps from (A) → (F) complete a catalytic cycle for nucleation. These energetics suggest that Co is the best catalyst for nucleation while Pt is almost as good as Co. Ni is a little worse than Co and Pt. Cu has an s^1d^{10} configuration so that it bonds to a single carbon atom for structures (A) and (E), leading to less stabilization of the new ring in (B) and (F). We conclude that Cu is the worst case for nucleation of nanotube among those metals.

(B) Growth of Nanotubes. To grow the nucleated structure into single-walled nanotubes, we must add carbons to form the six-member rings of the sidewall while avoiding the pentagonal rings that would tend to close up the tube. C_2 can add on to the edge of the nanotube either perpendicular or parallel to the growth edge. Parallel addition forming hexagon rings is 1.12 eV energetically more favorable than perpendicular addition forming pentagon rings. However, when two C_2 species are added to two adjacent sites, the perpendicular additions will become energetically more favorable than the parallel additions. As shown in Figure 1, two adjacent perpendicular additions (pathway (D)) lead to a defect with a new hexagon and two pentagon rings (called the 5,5,6,6 defect), while two adjacent parallel connections lead (pathway (C)) to two hexagon rings. Consequently, pathway (D) leads to closure of the nanotube tip since it leads to formation of additional similar defects. In contrast, following pathway (C), the growth will continue since no defects are formed. The calculations show that without a metal pathway (D) is 1.31 eV more favorable than pathway (C). Therefore, in the absence of metal atoms nanotube growth will quickly terminate by closing the open end needed for growth. Thus the 5,5,6,6 defects play a more important role than isolated pentagon rings.

The catalytic atom must be able to diffuse along on the edge or on the wall of the nanotube to anneal the growth defects before they can cause closure. Figure 3 indicates how a catalytic atom anneals the defect. After the catalytic atom attaches to the edge of the nanotube growth front to form species (A), it can move along the defect to form (B) and then insert into the defect to form species (C) in step (1). An incoming C_2 species can be attracted to the catalytic atom to form (D), subsequently releasing the metal atom and forming species (E) in step (2). The result of these two steps is that the catalytic atom moves out from the defect and adds a C_2 to build a hexagon ring. To complete the catalytic cycle, another C_2 is added to form species (F), which rearranges

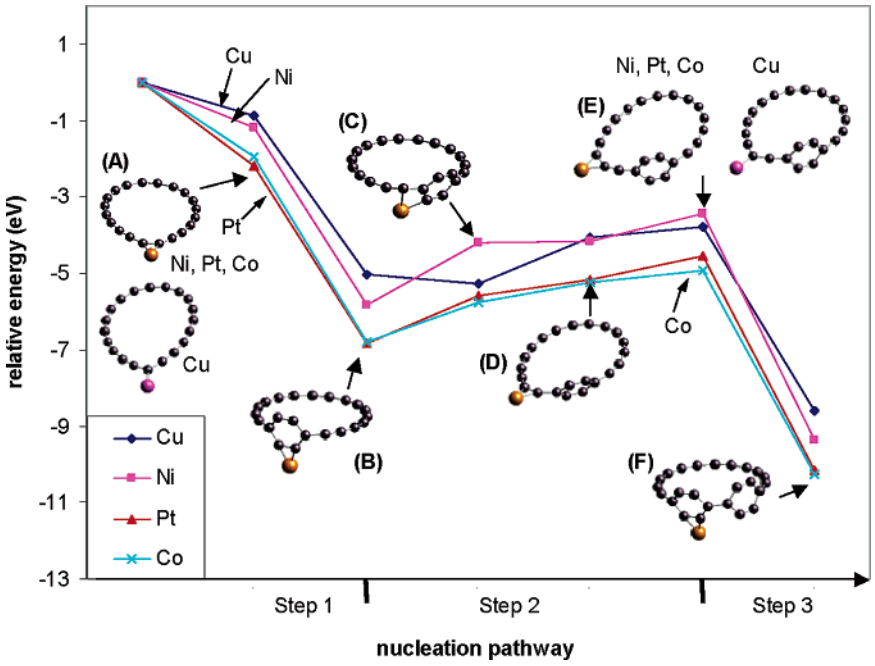

Figure 2. The catalytic cycle at the nucleation stage of SWCN growth (Path B in Figure 1). Starting with a carbon ring we first add a metal to form species (A). Step 1: C_2 addition to the carbon ring to form a six-membered ring at a metal-activated C═C bond. Step 2: Metal atom migrates along the carbon ring to position itself to an isolated C═C bond. Step 3: C_2 addition to the carbon ring to form a six-membered ring at the metal-activated C═C bond. The diagnostic for a successful nucleation is ΔE from (A) to (E). Shown are the energetics for four different metals.

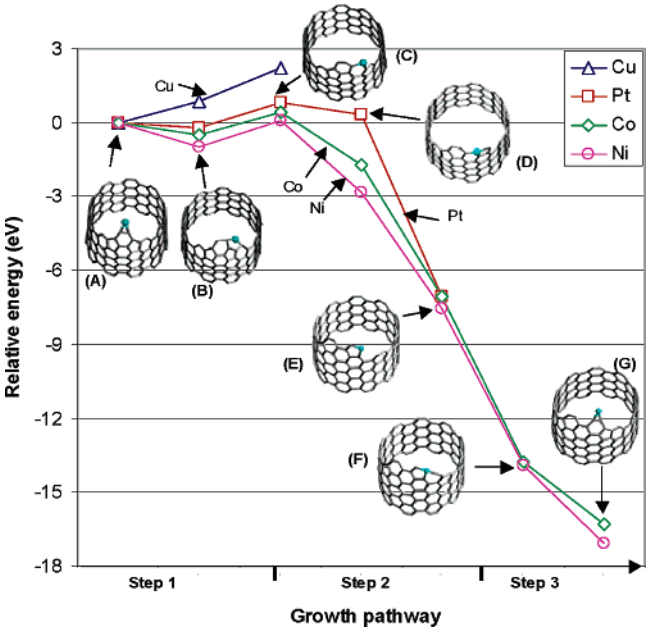

Figure 3. Catalytic circle for the growth stage of SWCN (Path E of Figure 1). Species (A) has a (5,5,6,6) defect which, without metal, would tend to close the nanotube as in Path D of Figure 1. Step 1: Moving the metal atom from (B) to (C) eliminates one 5-ring defect, the critical step in the repair mechanism. Step 2: A C_2 adds on the growth edge and releases the metal from the defect. Step 3: Metal migrates along the edge and assists another C_2 addition on to another cycle. The diagnostic for a successful G-DR is ΔE from species (A) to (C). Shown are the energetics for four different metals.

into species (G) in step (3). This catalytic cycle can continue to grow the bucky tube. As shown in Figure 3, our results indicate that Ni, Co, and Pt lead to favorable energetics for this catalytic cycle, but Cu does not. Because steps from (C) to (G) involve C_2 addition, which is quite favorable energetically, step (1) from (A) to (C), which involves only rearrangement of the bound metal atoms with the edge defect, will be the key step in determining the efficiency of various catalyst atoms. Comparing Ni, Co, and Pt at step (1) from species (A) to (C), we see that Ni should be best for annealing the defect (rearrangement energy of only 0.065 eV). Next best is Co (requiring 0.43 eV), followed by Pt with a barrier of 0.81 eV. Poorest is Cu, which because of its s^1d^{10} structure can form only one bond with the edge, leading to the largest barrier of 2.22 eV to insert into a defect to set up multiple bonds. We expect that Cu will poison growth since it would block the forthcoming annealing. Therefore, we conclude the catalytic efficiency for the growth stage is Ni > Co > Pt ≫ Cu. Indeed this order is exactly the same as deduced from experiment.[4] This suggests that the ability to maintain growth is more important than nucleation for mono-metal-catalyzed growth.

(C) Mechanism for Bimetallic Catalysts. We assume that the number of nanotubes is determined by the efficiency of the nucleation stage, while the length of the nanotubes is determined by the effectiveness of the catalytic growth with defect repair stage. Both stages affect the yield of nanotubes. Since the growth and nucleation stages involve different chemical properties, it is likely that the best catalyst for one might be different for the other. Thus we propose that the mechanism to explain the extraordinary improvement of SWCN production using bimetallic catalysts (10 to 100 times yield higher than the best monometallic catalyst) is that one metal is responsible for nucleation while the other is

Table 1. Energetics for the Diagnostic Steps of the Nucleation and Growth Mechanisms (units: eV)[a]

	Nucleation							
	I		II		III		IV	
species (A) → species (F)	Cu	−8.61	Pd	−9.21	Pt	−10.15	Cr	−11.14
			Ni	−9.37	Co	−10.25	Mo	−11.24
			Fe	−9.64				
			Rh	−9.89				
	Growth							
	poorest		poor		good		best	
species (A) → species (C)	Cu	2.22	Pd	1.23	Co	0.43	Ni	0.064
			Rh	1.10	Mo	0.37	Fe	0.13
			Cr	1.10				
			Pt	0.81				
	Poorest		Poor		Good		Best	

[a] Category IV is the best while category I is the worst.

responsible for G-DR. Since we find that the effectiveness for the nucleation stage is Co > Pt > Ni > Cu while the effectiveness for the growth stage is Ni > Co > Pt > Cu, we conclude that the mixture of Co and Ni would be the best catalysts for growth, followed by Ni mono-metal and then Pt. Of course the worst would be Ni mixed with Cu where Cu is expected to poison the catalyst. These conclusions are in exact agreement with experimental results.[4]

(D) Design of New Catalysts. To design better catalysts, we consider several additional metals: Cr, Fe, Rh, and Mo. Previous arc discharge experiments on Fe and Rh by themselves show poor growth rates, while Mo by itself does not work.[16,17] To simplify the evaluation, we choose several key structures in the nucleation and G-DR stages, i.e., species (A) and (F) in Figure 2 and species (A) and (D) in Figure 3. Table 1 summarizes our results. We rank Rh, Pd, Cr, Mo along with Ni, Co, Pt, and Cu by comparing the energetics of these key structures for nucleation and G-DR. Among all eight candidates, the poorest at nucleation and G-DR catalyst is Cu, which likely would acts as a poison to growth. This may explain why all attempts at bimetallic catalysts using Cu did not work (e.g., Ni+Cu and Co+Cu[4]). Therefore, a new catalyst should not include any Cu component.

We find that the best catalyst for nucleation is Mo followed by Cr, and then Co, Pt and then Rh, Fe, Ni, and Pd. However, the best growth catalyst is still Ni, followed by Fe and then Mo and Co. Therefore, we predict that the best catalyst for SWCN growth is Ni+Mo. Combining the predictions for nucleation and growth, these results suggest the following sequences of effectiveness:

$$\text{Ni+Mo} > \text{Ni+Cr} > \text{Ni+Co} > \text{Ni+Pt} > \text{Ni+Rh} > \text{Ni+Fe} > \text{Ni} > \text{Fe}$$

$$\text{Fe+Mo} > \text{Fe+Cr} > \text{Fe+Co} > \text{Fe+Pt} > \text{Fe+Rh} > \text{Fe}$$

$$\text{Ni+Mo} > \text{Fe+Mo} > \text{Co+Mo} > \text{Co}$$

Although there is less data about bimetallic catalysts for nanotube growth, our predictions lead exactly to the sequence Ni+Co > Ni+Pt > Ni > Ni+Cu established experimentally in ref 4 and to the sequence Ni+Co > Ni+Fe ~ Ni ≫ Fe established experimentally in ref 11 (we find that Ni + Fe should be slightly better than Ni alone, but the experiments report that they are similar). Indeed an experiment shows that Ni+Cr is more efficient than Ni alone for arc discharge growth of carbon nanotubes.[18] No experiments have been reported for the combinations Ni+Mo, Fe+Mo, and Co+Mo, which we expect to be the best catalysts. Some CVD experiments did find that Mo impurities enhance the yield of nanotubes combined with Fe or Co.[19,20] But this may not be relevant since the mechanism for CVD production of SWCN (likely involving nucleation and growth on the solid surface) is quite different than the gas phase growth for laser vaporization we are considering. On the other hand, our predicted preferences for different metals are reasonably consistent with CVD experiments, suggesting that there may be similar processes in both growth situations.

Lee et al.[9] discussing the mechanism for Ni acting alone, suggested that Ni migrates along the growth edge to prevent tube closure by eliminating pentagons as they form. They did not show why Ni would be better at this than other atoms. Our proposed growth stage is similar except that we conclude that the critical defect which must be removed is the 5,5,6,6 defect, which, as discussed above, is much more stable than isolated five-member rings and hence more difficult to eliminate. In addition, we showed that Ni is much better than other atoms. Of course in addition to the defect repair stage that is important to growth, our mechanism also accounts for nucleation.

Another mechanism proposed by Andriotis et al.[21] assumes that Ni atom repairs defects in the nanotube, binds to the defect, and then catalyzes the incorporation of a gas phase carbon atom to anneal the Ni-stabilized defects, freeing the Ni atom to be available to migrate to a new defect site. They did not explain why Ni is better than other atoms. Because a free carbon atom is much more active than metal atoms, we expect that replacing a metal atom in the carbon nanotube by free carbon atoms is energetically favorable for most metals. Thus, the Andriotis mechanism does not explain the observed huge difference in catalytic behavior between Ni, Co, Pt, and Cu, the last of which has no nanotube yield.

In summary, we propose a reasonable catalytic mechanism for the growth of carbon nanotubes that explains the observations on both monometallic and bimetallic catalytic effects on the basis of steps based on atomistic quantum calculations. Thus, our two stage mechanism explains that the monometallic catalytic efficiency is in the sequence Ni > Co > Pt ≫ Cu and also explains that the bimetallic catalytic efficiency is sequenced as Ni+Co > Ni+Pt > Ni > Ni+Cu. These results agree with experiment.[4,11] In addition, we used the two-stage mechanism to consider several systems not previously studied. We conclude that Ni+Mo and Cr+Ni should be even more efficient than the current catalysts and that Fe+Mo and Co+Mo might also be good catalysts.

Acknowledgment. This work was supported by an NSF-NIRT grant. The facilities of the Materials and Process

Simulation Center (MSC) used in these studies were funded by DURIP (ARO and ONR), NSF (CTS and MRI), and a SUR Grant from IBM. In addition, the MSC is funded by grants from ARO-MURI, NIH, Chevron Texaco, General Motors, Seiko-Epson, the Beckman Institute, Asahi Kasei, and Toray Corp.

References

(1) Iijima, S.; Ichihashi, T. *Nature (London)* **1993**, *363*, 603.
(2) Bethune, D. S.; Kiang, C. H.; Devries, M. S.; Gorman, G.; Savoy, R.; Vazquez, J.; Beyers, R. D. *Nature (London)* **1993**, *363*, 605.
(3) Thess, A.; Lee, R.; Nikolaev, P.; Dai, H. J.; Petit, P.; Robert, J.; Xu, C. H.; Lee, Y. H.; Kim, S. G.; Rinzler, A. G.; Colbert, D. T.; Scuseria, G. E.; Tomanek, D.; Fischer, J. E.; Smalley, R. E. *Science* **1996**, *273*, 483.
(4) Guo, T.; Nikolaev, P.; Thess, A.; Colbert, D. T.; Samlley, R. E. *Chem. Phys. Lett.* **1995**, *243*, 49.
(5) Cheng, H. M.; Li, F.; Su, G.; Pan, H. Y.; He, L. L.; Sun, X.; Dresselhaus, M. S. *Appl. Phys. Lett.* **1998**, *72*, 3282.
(6) Dai, H. J.; Kong, J.; Zhou, C. W.; Franklin, N.; Tombler, T.; Cassell, A.; Fan, S. S.; Chapline, M. *J. Phys. Chem. B* **1999**, *103*, 11246.
(7) Cheung, C. L.; Kurtz, A.; Park, H.; Lieber, C. M. *J. Phys. Chem. B* **2002**, *106*, 2429.
(8) Charlier, J. C.; Iijima, S. *Top. Appl. Phys.* **2001**, *80*, 55.
(9) Lee, Y. H.; Kim, S. G.; Tománek, D. *Phys. Rev. Lett.* **1997**, *78*, 2393.
(10) Kiang, C. H.; Goddard, W. A., III; Beyers, R.; Salem, J. R.; Bethune, D. S. *J. Phys. Chem. Solids* **1996**, *57*, 35.
(11) Puretzky, A. A.; Geohegan, D. B.; Fan, X.; Pennycook, S. J. *Appl. Phys. A* **2000**, *70*, 153.
(12) Hua, X.; Cagin, T.; Che, J.; Goddard, W. A. *Nanotechnology* **2000**, *11*, 85.
(13) Kiang, C. H.; Goddard, W. A. *Phys. Rev. Lett.* **1996**, *76*, 2515−2518.
(14) Jaguar 4.0, Schrodinger, Inc., Portland, OR, 1997.
(15) QM/MM calculation: the nanotube QM region is created by including metal atoms and the 5,5,6,6 defect (14 carbon atoms) plus three adjacent six-member rings where a metal atom will immigrate (12 carbon atoms). The ab initio total energy calculations were performed by using B3LYP. The atomic basis set used is LACVP* including relativistic effects for heavy atoms. The ground state was chosen by the structure with the lowest energy among different spin states of each structure. Dreiding force field was described in Mayo, S. L.; Olafson, B. D.; Goddard, W. A. *J. Phys. Chem.* **1990**, *94*, 8897.
(16) Saito, Y.; Nishikubo, K.; Kawabata, K.; Matsumoto, T. *J. Appl. Phys.* **1996**, *80*, 3062.
(17) Takikawa, H.; Kusano, O.; Sakakibara T. *J. Phys. D* **1999**, *32*, 2433.
(18) Bezmel'nitsyn, V. N.; Domantovski, A. G.; Eletski, A. V.; Obraztsova, E. V.; Pernbaum, A. G.; Prikhod'ko, K. E.; Terekhov, S. V. *Phys. Solid State* **2002**, *44*, 656.
(19) Yoon, Y. J.; Bae, J. C.; Baik, H. K.; Cho, S. J.; Lee, S. J.; Song, K. M.; Myung, N. S. *Physica B* **2002**, *323*, 318.
(20) Cassell, A. M.; Raymakers, J. A.; Kong, J.; Dai, H. J. *J. Phys. Chem. B* **1999**, *103*, 6484.
(21) Andriotis, A. N.; Menon, M.; Froudakis, G. *Phys. Rev. Lett.* **2000**, *85*, 3193.

NL048663S